

# Supramolecular Interaction of Molecular Cage and $\beta$ -Galactosidase: Application in Enzymatic Inhibition, Drug Delivery and Antimicrobial Activity

Avijit Mondal,<sup>[a]</sup> Imtiyaz Ahmad Bhat,<sup>[b]</sup> Subbaraj Karunakaran,<sup>[a]</sup> and Mrinmoy De<sup>\*[a]</sup>

Enzyme inhibitors play a crucial role in diagnosis of a wide spectrum of diseases related to bacterial infections. We report here the effect of a water-soluble self-assembled Pd<sup>II</sup><sub>8</sub> molecular cage towards  $\beta$ -galactosidase enzyme activity. The molecular cage is composed of a tetrapyrrolyl donor (L) and *cis*-[(en)Pd(NO<sub>3</sub>)<sub>2</sub>] (en = ethane-1,2-diamine) acceptor and it has a hydrophobic internal cavity. We have observed that the acceptor moiety mainly possesses the ability to inactivate the  $\beta$ -galactosidase enzyme activity. Kinetic investigation revealed the mixed mode of inhibition. This inhibition strategy was extended

to control the growth of methicillin-resistant *Staphylococcus aureus*. The internalization of the Pd(II) cage inside the bacteria was confirmed when bacterial solutions were incubated with curcumin loaded cage. The intrinsic green fluorescence of curcumin made the bacteria glow when put under an optical microscope. Furthermore, this curcumin loaded molecular cage shows an enhanced antibacterial activity. Thus, Pd<sup>II</sup><sub>8</sub> molecular cage is quite attractive due to its dual role as enzyme inhibitor and drug carrier.

## Introduction

Biomolecules are natural targets for the development of many inorganic drugs. Several small molecules,<sup>[1]</sup> nanomaterials and macromolecules<sup>[2]</sup> have been developed to target various biomolecules. Metal based supramolecular coordination architectures have been exploited extensively in catalysis, sensing, host-guest study, cavity induced unusual organic transformations, antimicrobial activity etc.<sup>[3]</sup> Similarly, their biomolecular interaction also opened up new avenues for biomedical research which include, sensing of biomolecules,<sup>[4]</sup> recognition of proteins,<sup>[5]</sup> recognition of nucleotide base,<sup>[6]</sup> anticancer therapy,<sup>[7]</sup> drug delivery<sup>[8]</sup> etc. Among them, recognition of protein is key to control a range of cellular processes, such as cellular signal transduction, protein antigen/antibody interaction and DNA transcription.<sup>[9]</sup> However, the effect of supramolecular coordination assemblies on protein is not well studied. Kamiya *et al.* have shown the interaction of saccharide coated M<sub>12</sub>L<sub>24</sub> molecular spheres with protein concanavalin-A and peanut agglutinin.<sup>[5]</sup> The polysaccharides present on the outer surface of the sphere help to recognize the protein surface of concanavalin A. Though M<sub>12</sub>L<sub>24</sub> sphere can recognize protein surface but the mode of interaction of the metallacage with protein and their kinetic behaviour have not been explored so far. To get insight about the interaction of

supramolecular coordination architecture with protein, we have chosen  $\beta$ -galactosidase ( $\beta$ -Gal) as a model protein and a water-soluble [Pd<sub>8</sub>L<sub>4</sub>]<sup>16+</sup> (1) molecular cage as metallasupramolecular architecture.

$\beta$ -Gal is a therapeutically relevant enzyme which catalyses the hydrolysis of  $\beta$ -D-galactoside to galactose and alcohol, which are the key sources to produce energy. It is a vital enzyme for the human body; the deficiency of which can cause galactosialidosis or Morquio B syndrome.<sup>[10]</sup>  $\beta$ -Gal is an essential enzyme for various microorganisms as well. Enhanced proliferation rate of various pathogenic bacteria like methicillin-resistant *Staphylococcus aureus* (MRSA), *Escherichia coli* (E. coli) rely on galacto-oligosaccharides which is formed through several enzymatic reactions catalysed by  $\beta$ -Gal.<sup>[11]</sup> Although there is a little difference exists between human  $\beta$ -Gal and bacterial  $\beta$ -Gal in their oligomerization state and domain organization, but the mode of action is nearly same. The loop region of  $\beta$ -domain 2 (residues 482–491) in human  $\beta$ -Gal execute the same role as the complementation loop of E. coli  $\beta$ -Gal. Moreover, the active site of human  $\beta$ -Gal is easily approachable from the bulk solvent whereas the active site of E. coli  $\beta$ -Gal is not easily accessible from the bulk solvent.<sup>[12]</sup> Hence, developing  $\beta$ -Gal inhibitor from E. coli benefits to tune the activity for various relevant application. In literature various small molecules have been reported as  $\beta$ -Gal inhibitor, such as L-ribose, D-galactose, D-galactonolactone etc.<sup>[13]</sup> Not only small molecules but also several nanomaterials have been developed to alter the enzymatic activity of  $\beta$ -Gal. Surface engineered gold nanoparticles,<sup>[14]</sup> MoS<sub>2</sub> nanosheets,<sup>[15]</sup> ZnO nanoparticles<sup>[16]</sup> and positively charged graphene oxide (GO)<sup>[17]</sup> have been used to tune the activity of  $\beta$ -Gal. By controlling the activity of  $\beta$ -Gal, bacterial growth can also be controlled as reported by Kotov *et al.*<sup>[16]</sup> However, to the best of our knowledge, metal based supramolecular coordination architectures have not yet been

[a] A. Mondal, S. Karunakaran, Dr. M. De  
Department of Organic Chemistry, Indian Institute of Science  
Bangalore 560012 (India)  
E-mail: md@iisc.ac.in

[b] I. A. Bhat  
Department of Inorganic and Physical Chemistry  
Indian Institute of Science, Bangalore 560012 (India)

Supporting information for this article is available on the WWW under  
<https://doi.org/10.1002/cbic.202100008>

explored as  $\beta$ -Gal enzyme inhibitor. Compared to existing systems, metallasupramolecular architecture-based inhibitors possibly hold many other advantages. Not only we can tune the surface property at the molecular level through the judicious selection of metals/ligands but also their high positive charges, large surface area, and high water solubility provide an attractive means to control the activity of enzyme.

We report here our study on the interaction of a water soluble metallasupramolecular  $[\text{Pd}_8\text{L}_4]^{16+}$  cage (1) with  $\beta$ -Gal (Figure 1). The cage 1 was constructed<sup>[18]</sup> employing a symmetrical tetrapyridyl donor (L) with *cis*- $[(\text{en})\text{Pd}(\text{NO}_3)_2]$  (en = ethane-1,2-diamine) acceptor. To our surprise, we have observed that the acceptor moiety is mainly responsible for enzyme inhibition. We have studied the mode of interaction of 1 with  $\beta$ -Gal through kinetic measurements. Also, inspired by the work of Kotov *et al.*,<sup>[16]</sup> we have extended our strategy to control the bacterial growth. The study revealed that the molecular cage 1 has higher antibacterial activity compared to the precursor building block *cis*- $[(\text{en})\text{Pd}(\text{NO}_3)_2]$  against methicillin-resistant *Staphylococcus aureus* (MRSA) bacteria. We expected that the cage 1 would penetrate the cell more efficiently and inhibit  $\beta$ -Gal in the cytosolic environment. In order to support the internalization of the cage 1 inside the bacteria cell, we have used curcumin as a trapping reagent. Curcumin is insoluble in water, but the hydrophobic cavity of  $\text{Pd}_8\text{L}_4$  cage (1) offers to encapsulate curcumin to form the water-soluble inclusion complex ( $1 \subset \text{curcumin}$ ).<sup>[18]</sup> Thus, the inclusion complex  $1 \subset \text{curcumin}$  can be used for targeting the enzyme and as a drug carrier simultaneously.

## Results and Discussion

### Synthesis and characterization of $\text{Pd}_8^{\text{II}}$ molecular cage

First, we synthesised the water-soluble tetrafacial  $\text{Pd}_8\text{L}_4$  coordination cage 1 by self-assembly of the symmetric tetrapyridyl donor L with a  $90^\circ$  acceptor M [where  $\text{M} = \text{cis}-(\text{en})\text{Pd}(\text{NO}_3)_2$ ; en = ethane-1,2-diamine] following the reported procedure (Fig-

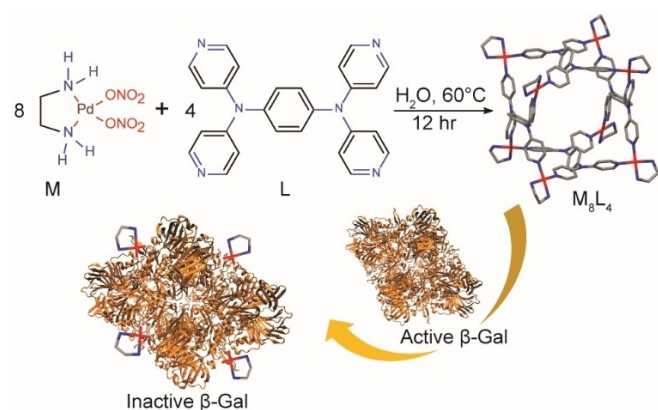


**Figure 1.** Synthesis of  $[\text{Pd}_8\text{L}_4]^{16+}$  molecular cage (1) and the inhibitory interaction with  $\beta$ -Gal enzyme.

ure 1).<sup>[18]</sup> The molecular cage 1 was characterized by  $^1\text{H}$  NMR, ESI-MS spectrometry to reconfirm the structure and purity before the biological study.<sup>[18]</sup> Four ligands (L) are present along the four walls of the square-barrel and are connected together by eight acceptor units present along the edges to form the overall square barrel structure. The cage possesses a hydrophobic internal cavity with dimensions of  $12.2 \times 12.2 \times 15.3 \text{ \AA}^3$ . Also, the presence of the eight *cis*- $[(\text{en})\text{Pd}(\text{NO}_3)_2]$  groups in cage 1 makes it highly water soluble and cationic (with +16 charge) in nature. Due to its cylindrical and barrel-shaped structure, the molecular cage 1 possesses windows similar to its cavity size which makes it suitable for the easy ingress and egress of the hydrophobic drug molecules. In biological systems, barrel-shaped molecules such as  $\beta$ -barrel proteins are known for diffusing the small molecules and ions across cell membranes.<sup>[19]</sup> In this regard, various barrel-shaped molecules having large intrinsic cavities have been reported in literature with potential applications in biology.<sup>[20]</sup>

### $\beta$ -Gal activity assay and inhibition kinetics

$\beta$ -Gal is a large tetrameric protein which has overall negatively charged surface.<sup>[14]</sup> The active site of the  $\beta$ -Gal contains Glutamic acids residues which are mainly responsible for enzyme catalysis. The most possible mode of inhibition is due to the binding of the cage to  $\beta$ -Gal through electrostatic interaction followed by coordination Pd complex with amino acid residues at active site. As the active site of the  $\beta$ -Gal has negatively charged residues and the cage is overall positively charged, so there is also a possibility of blocking the active site of  $\beta$ -Gal by cage. Not only into the active site but also cage can bind to the surface of the enzyme and thereby altering its enzymatic activity as reported by using other macromolecules.<sup>[21]</sup> To support the above hypothesis, activity assays were performed to test the ease of inhibition by cage 1 using *o*-nitrophenyl- $\beta$ -D-galactopyranoside (ONPG) as a chromogenic substrate (Figure 2a). The experiment was carried out by pre-incubating 0.5 nM  $\beta$ -Gal with variable concentrations of the cage 1 (ranging from 0 to 310 nM) in 5 mM sodium phosphate buffer (pH 7.4) for 30 min. The enzymatic activity was monitored from the rate of hydrolysis of ONPG. The activity of  $\beta$ -Gal in the absence of 1 was taken as control. The activities in the presence of the cage 1 were normalized after subtracting the blank (without enzyme). The enzymatic activity was reduced to  $\sim 10\%$  when the concentration of 1 reached 310 nM (Figure 2b). But in case of control experiment with *cis*- $[(\text{en})\text{Pd}(\text{NO}_3)_2]$  complex shows a similar extent of enzymatic activity inhibition (since one cage is formed by 8 *cis*- $[(\text{en})\text{Pd}(\text{NO}_3)_2]$  components) (Figure 2d). The  $\text{IC}_{50}$  value for the cage 1 is 53.8 nM (Figure 2c) whereas the  $\text{IC}_{50}$  value for the Pd acceptor is 925 nM (figure 2d). This suggest that cage is better inhibitor than only Pd-acceptor possibly due to the higher local concentration. We have carried out the same experiment in 0.01% triton X-100 to verify the possibility of aggregation induced inhibition (supporting information, Figure S1). The experimental data shows nearly closer value of  $\text{IC}_{50}$  in PBS

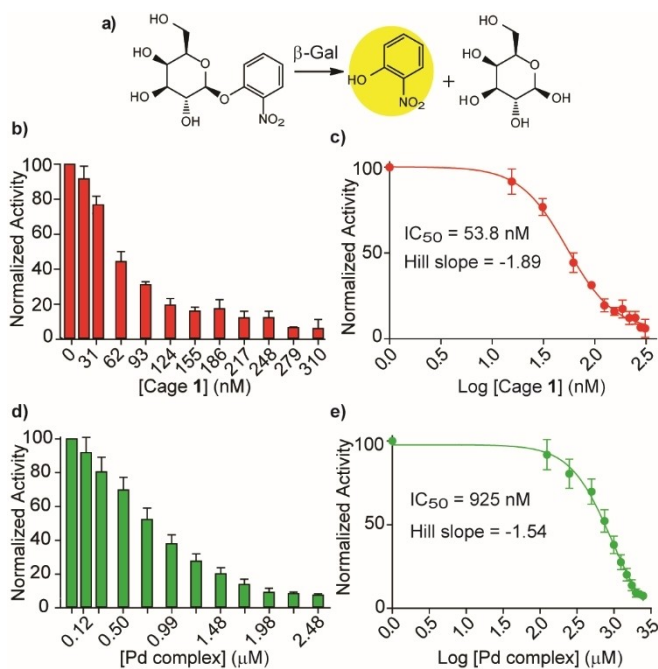


**Figure 2.** (a) Scheme of ONPG hydrolysis with  $\beta$ -Gal in 5 mM sodium phosphate buffer (pH 7.4) using ONPG as a substrate. (b) Normalized activity of  $\beta$ -Gal (0.5 nM) as a function of different concentrations of cage 1. (c)  $IC_{50}$  for cage 1 and hill slope. (d) Normalized activity of  $\beta$ -Gal (0.5 nM) as a function of different concentrations of *cis*-[(en)Pd(NO<sub>3</sub>)<sub>2</sub>] complex. (e)  $IC_{50}$  for *cis*-[(en)Pd(NO<sub>3</sub>)<sub>2</sub>] complex and hill slope.

(53.8 nM) and in 0.01% triton X-100 (51.8 nM), which excludes the possibility of aggregation induced inhibition. The close value of  $IC_{50}$  of free complex and the cage suggests that the cage 1 in the presence of  $\beta$ -Gal was disassembled and each acceptor unit present in the cage played a key role to inhibit the activity of  $\beta$ -Gal. Even though it was well established that the active site of  $\beta$ -Gal (His-418) is highly responsible for metal ion binding and hence has a direct effect on enzymatic activity,<sup>[22]</sup> however there are no metal complex based inhibitor reported so far.

Understanding the mode of enzyme inhibition helps to determine the nature of the interaction with cage 1. The enzyme velocity data as a function of substrate (S) concentration at different fixed concentrations of 1 was used to calculate the inhibition constant ( $K_i$ ). The data were fitted according to nonlinear regression using Graph-Pad Prism 5 software. The equation used to determine the velocity (V) of an enzymatic reaction in the presence of an inhibitor (I) is:

$$V = \frac{V_{max} [S]}{[S] \left(1 + \frac{I}{\alpha K_i}\right) + \left(1 + \frac{I}{K_i}\right)}$$

The calculated value of  $\alpha$  from the above equation is important to determine whether the mode of interaction is competitive, non-competitive, or uncompetitive.<sup>[23]</sup> When the value of  $\alpha \gg 1$ , it indicates competitive inhibition. In competitive inhibition, the inhibitor binds exclusively to the active site

of the enzyme. When the value of  $\alpha = 1$ , inhibition is non-competitive. In this kind of inhibition, the inhibitor does not affect the binding of substrate to the enzyme, instead, it binds with the enzyme substrate complex and free enzyme with equal affinity. A value of  $\alpha \ll 1$  indicates uncompetitive inhibition. In uncompetitive inhibition, inhibitor binds to the enzyme-substrate complex exclusively. By using the above expression, the curve fitting analysis gave  $\alpha$  value ranging from 1.34 to 2.44 which could be due to the mixed mode of inhibition (supporting information, Figure S2). The mode of inhibition can also be assessed by using the Lineweaver-Burk plot (Figure 3b). From the curve fitting analysis, we observed the value of  $K_i$  to be 95.34 nM. Compared to other nanomaterial based inhibitors (e.g. 0.72  $\mu$ M for ZnO nanopyramid<sup>[16]</sup>) and conventional inhibitors (e.g. 1  $\mu$ M for phenylethyl thio- $\beta$ -D-galactoside (PETG),<sup>[24]</sup> 24 mM for D-galactose,<sup>[24]</sup> 0.24 mM for L-ribose,<sup>[24]</sup> 0.7 mM for D-galactonolactone)<sup>[24]</sup> cage 1 exhibits very high enzymatic inhibition without any effect on secondary structure (Supporting Information, Figure S3).

### Antibacterial activity against MRSA

As the  $\beta$ -Gal is highly responsible for bacterial growth,<sup>[11]</sup> cytosolic inhibition of its activity can control the growth of various microorganisms. Applying this hypothesis, earlier small molecule such as ginkgolic acid (C15:1)<sup>[25]</sup> and ZnO nanopyramids<sup>[16]</sup> were used for antibacterial activity. Considering those reports, the cage 1 or the *cis*-[(en)Pd(NO<sub>3</sub>)<sub>2</sub>] complex

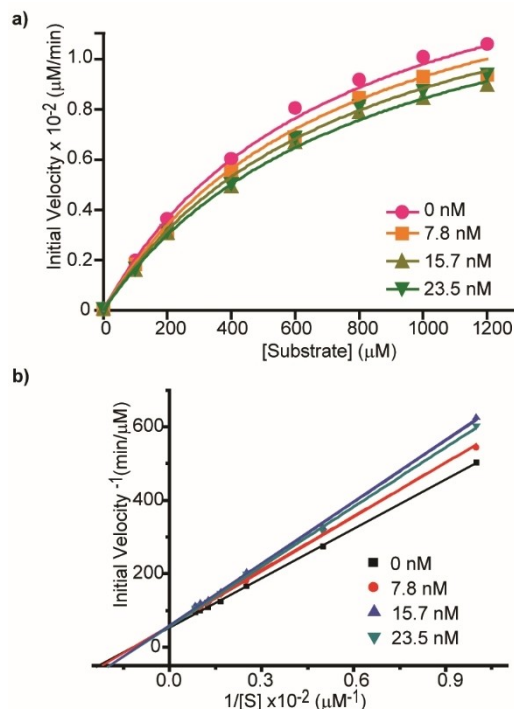


**Figure 3.** (a) Enzyme velocity as a function of substrate concentration at various fixed concentration of cage 1. 2.5 nM  $\beta$ -gal concentration was maintained throughout the experiment. (b) Lineweaver-Burk plot.

might be expected to show antibacterial effects. We have carried out the growth kinetics of MRSA bacteria in presence of various concentration of cage 1 and it shows MIC at 0.1 mM concentration (Figure 4a). Similarly, we have also explored the effect in case of gram-negative bacteria. For that purpose, we have considered *P. aeruginosa* (PA) and we have observed almost equally effective antimicrobial activity (Figure 4b). In order to test the bacteria killing efficacy of cage 1 and Pd complex, we have checked the colony forming ability of MRSA bacteria in agar plate. MRSA bacteria having OD 0.01 were incubated at 37 °C for 5–6 hours with different concentrations of cage 1 (ranging from 0.1 mM to 0.25 mM) and *cis*-[(en)Pd(NO<sub>3</sub>)<sub>2</sub>] complex (ranging from 0.8 mM to 2 mM; 8 times compared to cage 1 concentration). The bacterial solution without the cage 1 or Pd acceptor complex was taken as control. After incubation, bacterial solutions were diluted 100 times and 10 μL of the solution streaked on agar plate to check the bactericidal efficiency of cage 1 and *cis*-[(en)Pd(NO<sub>3</sub>)<sub>2</sub>] complex (Figure 4). There is a significant reduction in colony formation in the presence of cage 1 (Figure 4c); however, the *cis*-[(en)Pd(NO<sub>3</sub>)<sub>2</sub>] complex failed to show any significant reduction in colony formation even at 2 mM concentration (Figure 4d). The ligand (L) also did not show any antibacterial effect (Supporting Information, Figure S4).

Based on the above observation, we can conclude that, even though the *cis*-[(en)Pd(NO<sub>3</sub>)<sub>2</sub>] complex is responsible for β-Gal enzyme inhibition, it is not suitable for bacterial cell wall and plasma membrane penetration. Whereas the bacteria killing efficiency of cage 1 suggests that the self-assembled cage is suitable for cell internalization, possibly due to the presence of amine bound cationic acceptor on the corners (with +16 charge). Once the cage 1 is internalized inside the bacteria

cytosol, it inhibits the β-Gal and thus prevents the bacterial growth. This is confirmed by checking the amount of active β-Gal remained inside the bacteria after treating with cage 1 and *cis*-[(en)Pd(NO<sub>3</sub>)<sub>2</sub>] complex (Supporting Information, Figure S5). This was done by using treated bacteria cell lysates. It was observed that bacteria treated with cage 1 possesses very less amount of active β-Gal in cell lysates compared to the bacteria treated with *cis*-[(en)Pd(NO<sub>3</sub>)<sub>2</sub>] complex. This confirms the better internalization of cage molecule compare to the acceptor building blocks. The better internalization ability of 1 through the bacterial cell membrane followed by disintegration by enzymes also can be used as a carrier of various water insoluble drug molecules. In order to further support the better internalization of the cage molecule and carrier of hydrophobic drugs we have used curcumin as a trapping agent. Curcumin, the core ingredient of turmeric, is known to have a broad range of pharmacological properties and is a popular antimicrobial, antidiabetic, anti-inflammatory, anticancer, and antioxidant agent.<sup>[26]</sup> Also, the intrinsic green fluorescence of curcumin was used as an optical biomarker.<sup>[27]</sup> Though curcumin has a wide range of applications, but its poor solubility in water limits its bioavailability and pharmacological potential.<sup>[28]</sup> We have shown previously that the hydrophobic interior of the cage 1 can efficiently encapsulate curcumin<sup>[18]</sup> and we found that, 15 μM cage 1 can encapsulate 16.3 μM of curcumin (Supporting Information). Following the similar method, the internalization of 1 within the bacterial cell was confirmed when the bacterial solution was incubated with curcumin loaded cage (1⊂curcumin). The intrinsic green fluorescence of curcumin made the bacteria fluoresce when analysed under the optical microscope (Figure 5a).

However, the bacteria treated only with curcumin did not show any fluorescence (Figure 5b). This indicates that the cage 1 is internalized in bacterial cells followed by its disintegration inside the bacteria to release the curcumin in cytosol. As the sparingly water-soluble curcumin has antibacterial activity, we have also tested the effect of the curcumin loaded cage system (1⊂curcumin) on the growth of MRSA bacteria. As speculated, the antibacterial efficacy of 1⊂curcumin system was found to exhibit higher compared to the only cage 1 molecule. While checking the antibacterial efficacy of 1⊂curcumin, we have found that 1⊂curcumin shows higher antibacterial activity compared to cage 1 alone. Though there were a few colonies noted at 0.25 mM cage concentration (Figure 4c), but no bacterial colony formation was observed at this concentration for the curcumin loaded cage (1⊂curcumin) (Figure 5c). In a control experiment only with curcumin, an uncountable number of colonies were formed (Figure 5d) (curcumin concentration was varied from 0.16 mM to 0.27 mM). This observation further established that the poor solubility and hence less bioavailability of curcumin is inefficient for therapeutic applications. But cage 1 forms inclusion complex (1⊂curcumin) which enhances the effective solubility and efficiently internalized by bacteria cells. After internalization, the cage was disintegrated inside the cell and released the curcumin drug that led to higher antibacterial effect. In our previous report we have demonstrated that the toxicity of 1⊂curcumin as well as cage 1

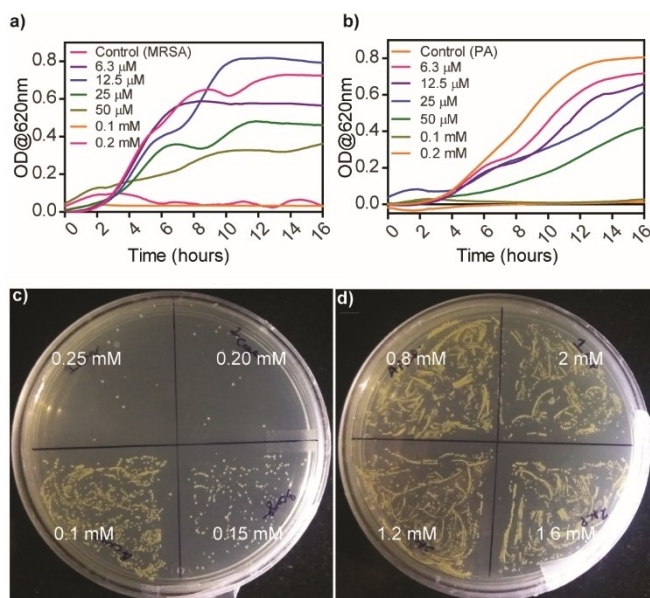


**Figure 4.** Bacterial growth curve in presence different concentration of cage 1 (a) MRSA (b) PA. Colony-forming ability of MRSA after treating with: (c) different concentrations of cage 1; (d) different concentrations of *cis*-[(en)Pd(NO<sub>3</sub>)<sub>2</sub>] complex.

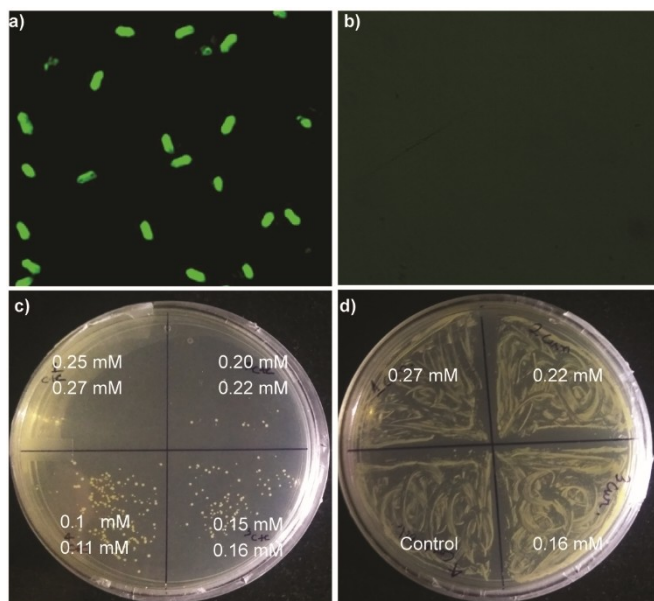


**Figure 5.** Fluorescence imaging of MRSA bacteria incubated with (a) curcumin loaded cage (1Ccurcumin) and (b) only curcumin. (c) Colony-forming ability of MRSA after treating with different concentrations of curcumin loaded cage (1Ccurcumin) (top concentration is for cage and bottom concentration is for loaded curcumin) and (d) Control and different concentrations of only curcumin.

is very low based on cellular toxicity assay using HeLa cells.<sup>[18]</sup> Hence development of this kind of cage system is always attractive for drug loading purpose. By changing the building block of cage system, the internal cavity size can be tuned to encapsulate various hydrophobic drug of comparable sizes. Although the cage system is very attractive for drug loading, it has few limitations as well. A small internal cavity cannot encapsulate the drugs of bigger sizes. Moreover, the presence of a specific enzyme is one of the criteria to release the drug inside the bacteria.

## Conclusion

In summary, we have explored the biomolecular interaction of a Pd<sub>8</sub>L<sub>4</sub> supramolecular coordination cage 1 with β-Gal enzyme. We observed that in presence of the β-Gal enzyme the cage 1 disintegrates and the *cis*-[(en)Pd(NO<sub>3</sub>)<sub>2</sub>] building block of the cage is mainly responsible for mixed mode enzyme inhibition. This is the first report of a metal complex based β-Gal inhibition. Also, we observed the cage 1 can be internalized inside the bacteria more efficiently compared to the acceptor building unit and exhibits higher antibacterial activity against MRSA bacteria. Moreover, the hydrophobic interior of the water-soluble cage helps to encapsulate hydrophobic antibacterial drug curcumin and can offer as a potential drug carrier. Combining the cellular internalization, enzymatic inhibition and hydrophobic drug encapsulation, curcumin loaded cage 1 exhibits better antibacterial activity compared to the cage alone.

## Experimental Section

**Materials and methods:** β-Galactosidase (from *Escherichia coli*), *o*-nitrophenyl-β-D-galactopyranoside (ONPG) and curcumin were purchased from Sigma. Bruker 400 MHz NMR instrument was used to record NMR spectra. Agilent 6538 Ultra-High Definition (UHD) Accurate Mass Q-TOF spectrometer was used for ESI-MS experiments. Activity assays were done by using Thermo Scientific Varioskan Flash Multimode Reader (ultraviolet-visible measurement). JASCO, J-815 CD spectrometer was used to measure circular dichroism spectra. Bacterial optical density was measured by Eppendorf Bio Spectrometer UV-vis spectrometer. Bacterial imaging was performed by an Olympus IX73 microscope.

**Synthesis and characterization of Pd<sub>8</sub>L<sub>4</sub> cage 1:** Pd<sub>8</sub>L<sub>4</sub> molecular cage 1 was synthesized according to our earlier reported procedure.<sup>[18]</sup> Briefly, in a glass vial ligand L (21.4 mg, 0.05 mmol) and *cis*-[(en)Pd(NO<sub>3</sub>)<sub>2</sub>] (30 mg, 0.1 mmol) were taken and 1.5 mL of Millipore water was added to it. The suspension was sonicated for proper mixing and then heated at 60 °C with constant stirring for 12 h. The faint bluish solution formed was centrifuged to get the clear supernatant solution. Methanol was slowly diffused into the solution to obtain shining single crystals of 1 after 15 days. Isolated yield: 28.5 mg, 55%. IR:  $\nu$  (cm<sup>-1</sup>) = 3101, 1599, 1495, 1314, 1215, 1059, 824, 593. <sup>1</sup>H NMR (400 MHz, D<sub>2</sub>O):  $\delta$  = 8.51 (d, 32H), 7.85 (s, 8H), 7.46 (d, 32H), 7.24 (s, 8H) and 3.18 (s, 32H). ESI-MS (m/z) = 1268.0125 [1-3NO<sub>3</sub>]<sup>+3</sup>, 936.3440 [1-4NO<sub>3</sub>]<sup>+4</sup> and 603.9027 [1-6NO<sub>3</sub>]<sup>+6</sup>.

**Activity assay:** All the experiments were carried out in sodium phosphate buffer (pH 7.45) at 25 °C. For the enzyme inhibition studies, 0.5 nM of β-galactosidase was incubated with varying concentration of the molecular cage 1 (concentrations ranging from 0 to 310 nM) and [cis-(en)Pd(NO<sub>3</sub>)<sub>2</sub>] complex (concentrations ranging from 0 to 2.48 μM) for 30 minute in 96-well plate. After 30 minutes of incubation, the enzymatic hydrolysis reaction was initiated by adding 4.41 mM ONPG stock solution (final concentration 441 μM). The enzyme activity was monitored by estimating the formation of *o*-nitrophenolate anion from ONPG over a period of 3 hour at  $\lambda$  = 405 nm with a microplate reader (Thermo Scientific Varioskan Flash Multimode Reader (ultraviolet-visible measurement)). The assays were performed in triplicates. In parallel same experiments were carried out taking every other component except the enzyme and these blank values were subtracted from the experimental time points. All the concentration mentioned here are the final concentrations. The tetrapyridyl ligand is insoluble in water so it is not possible to carry out the control study with the ligand.

**Kinetic study:** To elucidate the mode of binding, and to calculate the inhibition constant (*K<sub>i</sub>*) β-galactosidase (2.5 nM) was incubated with various concentration of molecular cage 1 (0 nM, 7.8 nM, 15.7 nM and 23.5 nM). For each concentration of molecular cage 1 initial velocity was measured at various concentration of ONPG. The initial velocity was determined in all cases by the linear fitting of *o*-nitrophenolate anion (hydrolysis by-product) formation over the time intervals at  $\lambda$  = 405 nm. The experiments were performed in triplicates. All fittings were performed using GraphPad Prism 5, where the mixed-model inhibition equation (which is a general velocity equation) was used to calculate the inhibition constant *K<sub>i</sub>*. Mixed-model inhibition includes competitive, uncompetitive, and noncompetitive inhibition as special cases. The control plot gives the *K<sub>m</sub>* value of ONPG 728 μM. The reciprocals of enzymatic velocity enzyme velocity and substrate concentration plot is known as Lineweaver-Burk plot which helps to determine the mode of inhibition.

**Antimicrobial assays:** The antibacterial activity of the molecular cage 1, [cis-(en)Pd(NO<sub>3</sub>)<sub>2</sub>] complex, inclusion complex 1Ccurcumin

was tested against the growth of Methicillin Resistant *Staphylococcus aureus* (MRSA, USA300). The freeze-dried bacterial stock was revived on nutrient agar plates. Primary culture was then prepared by taking few colonies of bacteria from agar plate and culturing it in Luria broth media (LB, HiMedia – 20 g/L) overnight 37 °C for 10–12 h. For secondary culture 100 µL of primary culture was sub-cultured in 10 mL of fresh LB until it reaches to the mid-log phase ( $OD_{600nm} \sim 0.3$ ). The final optical density of the bacterial solution was adjusted to OD 0.01, which corresponds to  $10^6$  to  $10^7$  bacteria/mL and was used for the experiments. Now in different Eppendorf tube 100 µL of different concentration of molecular cage 1, [cis-(en)Pd(NO<sub>3</sub>)<sub>2</sub>] complex, inclusion complex 1Ccurcumin was added. To each Eppendorf tube 100 µL of bacterial suspension (OD 0.01) was added. Then the solutions were incubated at 37 °C, 150 rpm for 5–6 hours. Bacterial solution without the material was taken as control. After incubation, bacterial solutions were diluted 100 times and 10 µL of the solution streaked on agar plate to check the bactericidal efficiency of the cage, [cis-(en)Pd(NO<sub>3</sub>)<sub>2</sub>] complex and inclusion complex 1Ccurcumin. The antibacterial activity of curcumin was carried out following the same procedure, but the stock solution of curcumin was prepared in 10% DMSO (as curcumin is sparingly soluble in water).

**Curcumin encapsulation:** Curcumin molecule is a known potential drug molecule with many therapeutic uses. However, its very low solubility in water limits its therapeutic use. To increase the bioavailability of the curcumin drug, a water-soluble carrier vehicle is needed which can encapsulate it inside its hydrophobic cavity and delivers it to the desired target inside the cell. In this endeavour, the water-soluble cage 1 was used to encapsulate the curcumin in water to form the host-guest complex 1Ccurcumin. The host-guest 1Ccurcumin complex was obtained by following the literature procedure. To the 10 mg of cage 1 taken in 4 ml glass vial dissolved in 2 ml water, 2 mg of curcumin was added, and the suspension solution was allowed to stir for 24 h at room temperature. The clear yellow coloured aqueous solution of host-guest 1Ccurcumin was obtained by centrifugation after removal of undissolved curcumin.

**Imaging with curcumin loaded cage (1Ccurcumin):** The MRSA bacterial solution having OD 0.01 was prepared following the above-mentioned procedure. Then 100 µL of the bacterial solution was incubated at 37 °C separately with water soluble inclusion complex 1Ccurcumin (125 µM 1Ccurcumin) and with curcumin (135 µM) for 6 hours. After the incubation, bacterial samples were washed with PBS three times and then transferred to a glass slide for imaging. Olympus IX73 microscope was used for the imaging purpose.

## Acknowledgements

The authors would like to thank BRNS (37(2)/14/07/2017-BRNS) and SERB (CVD/2020/000855) for financial support. The authors would also like to thank Prof. Partha Sarathi Mukherjee from Inorganic and Physical Chemistry Department, IISc, Bangalore for providing the cage materials for this study.

## Conflict of Interest

The authors declare no conflict of interest.

**Keywords:** cage compounds · enzymatic inhibition · antibacterial activity · self-assembly · supramolecular chemistry

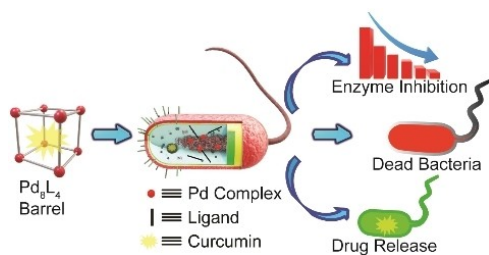
- [1] T. K. Ritter, C. H. Wong, *Angew. Chem. Int. Ed.* **2001**, *40*, 3508–3533; *Angew. Chem.* **2001**, *113*, 3616–3641.
- [2] A. S. Abd-El-Aziz, C. Agatemor, N. Etkin, *Biomaterials* **2017**, *118*, 27–50.
- [3] a) P. Howlader, P. Das, E. Zangrando, P. S. Mukherjee, *J. Am. Chem. Soc.* **2016**, *138*, 1668–1676; b) X. Yan, T. R. Cook, P. Wang, F. Huang, P. J. Stang, *Nat. Chem.* **2015**, *7*, 342–348; c) S. Bhattacharyya, M. Venkateswarulu, J. Sahoo, E. Zangrando, M. De, P. S. Mukherjee, *Inorg. Chem.* **2020**, *59*, 12690–12699; d) S. Bhattacharyya, S. R. Ali, M. Venkateswarulu, P. Howlader, E. Zangrando, M. De, P. S. Mukherjee, *J. Am. Chem. Soc.* **2020**, *142*, 18981–18989.
- [4] K. M. C. Wong, M. M. Y. Chan, V. W. W. Yam, *Adv. Mater.* **2014**, *26*, 5558–5568.
- [5] N. Kamiya, M. Tominaga, S. Sato, M. Fujita, *J. Am. Chem. Soc.* **2007**, *129*, 3816–3817.
- [6] M. Mounir, J. Lorenzo, M. Ferrer, M. J. Prieto, O. Rossell, F. X. Aviles, V. Moreno, *J. Inorg. Biochem.* **2007**, *101*, 660–666.
- [7] Y. Qin, L.-J. Chen, F. Dong, S.-T. Jiang, G.-Q. Yin, X. Li, Y. Tian, H.-B. Yang, *J. Am. Chem. Soc.* **2019**, *141*, 8943–8950.
- [8] B. Therrien, G. Suss-Fink, P. Govindaswamy, A. K. Renfrew, P. J. Dyson, *Angew. Chem. Int. Ed.* **2008**, *47*, 3773–3776; *Angew. Chem.* **2008**, *120*, 3833–3836.
- [9] a) B. A. Chrunyk, M. H. Rosner, Y. Cong, A. S. McColl, I. G. Otterness, G. O. Daumy, *Biochemistry* **2000**, *39*, 7092–7099; b) Z. Y. Zhang, R. A. Poorman, L. L. Maggiora, R. L. Heinrikson, F. J. Kezdy, *J. Biol. Chem.* **1991**, *266*, 15591–15594.
- [10] S. Okada, J. S. O'Brien, *Science* **1968**, *160*, 1002–1004.
- [11] D. H. Juers, B. W. Matthews, R. E. Huber, *Protein Sci.* **2012**, *21*, 1792–1807.
- [12] U. Ohto, K. Usui, T. Ochi, K. Yuki, Y. Satow, T. Shimizu, *J. Biol. Chem.* **2012**, *287*, 1801–1812.
- [13] R. E. Huber, R. L. Brockbank, *Biochemistry* **1987**, *26*, 1526–1531.
- [14] A. Verma, J. M. Simard, J. W. E. Worrall, V. M. Rotello, *J. Am. Chem. Soc.* **2004**, *126*, 13987–13991.
- [15] S. Karunakaran, S. Pandit, M. De, *ACS Omega* **2018**, *3*, 17532–17539.
- [16] S. H. Cha, J. Hong, M. McGuffie, B. Yeom, J. S. VanEpps, N. A. Kotov, *ACS Nano* **2015**, *9*, 9097–9105.
- [17] J. Li, L. J. Wu, S. S. Guo, H. E. Fu, G. N. Chen, H. H. Yang, *Nanoscale* **2013**, *5*, 619–623.
- [18] I. A. Bhat, R. Jain, M. M. Siddiqui, D. K. Saini, P. S. Mukherjee, *Inorg. Chem.* **2017**, *56*, 5352–5360.
- [19] a) R. E. Bishop, *Biochim. Biophys. Acta Biomembr.* **2008**, *1778*, 1881–1896; b) D. Yamashita, T. Sugawara, M. Takeshita, J. Kaneko, Y. Kamio, I. Tanaka, Y. Tanaka, M. Yao, *Nat. Commun.* **2014**, *5*, 4897.
- [20] E. G. Percastegui, T. K. Ronson, J. R. Nitschke, *Chem. Rev.* **2020**, *120*, 13480–13544.
- [21] S. van Dun, C. Ottmann, L.-G. Milroy, L. Brunsveld, *J. Am. Chem. Soc.* **2017**, *139*, 13960–13968.
- [22] D. H. Juers, B. Rob, M. L. Dugdale, N. Rahimzadeh, C. Giang, M. Lee, B. W. Matthews, R. E. Huber, *Protein Sci.* **2009**, *18*, 1281–1292.
- [23] A. A. Saboury, *J. Iran. Chem. Soc.* **2009**, *6*, 219–229.
- [24] D. H. Juers, S. Hakda, B. W. Matthews, R. E. Huber, *Biochemistry* **2003**, *42*, 13505–13511.
- [25] Z. Hua, C. Wu, G. Fan, Z. Tang, F. Cao, *BMC Biotechnol.* **2017**, *17*, 5.
- [26] a) S. C. Gupta, S. Prasad, J. H. Kim, S. Patchva, L. J. Webb, I. K. Priyadarsini, B. B. Aggarwal, *Nat. Prod. Rep.* **2011**, *28*, 1937–1955; b) R. K. Maheshwari, A. K. Singh, J. Gaddipati, R. C. Srimal, *Life Sci.* **2006**, *78*, 2081–2087; c) S. Z. Moghadamtousi, H. A. Kadir, P. Hassandarvish, H. Tajik, S. Abubakar, K. Zandi, *BioMed Res. Int.* **2014**, *2014*, 186864.
- [27] S. Shanmugaraju, B. la Cour Poulsen, T. Arisa, D. Umadevi, H. L. Dalton, C. S. Hawes, S. Estalayo-Adrián, A. J. Savyasachi, G. W. Watson, D. C. Williams, T. Gunnlaugsson, *Chem. Commun.* **2018**, *54*, 4120–4123.
- [28] S. Y. Teow, K. Liew, S. A. Ali, A. S. Khoo, S. C. Peh, *J. Trop. Med. Hyg.* **2016**, *2853045*.

Manuscript received: January 7, 2021

Revised manuscript received: March 31, 2021

Accepted manuscript online: April 4, 2021

Version of record online: ■■■, ■■■■



The effect of a water-soluble Pd<sub>118</sub> molecular cage towards  $\beta$ -galactosidase enzyme activity was studied. The cage disintegrates in the presence of the enzyme and inhibits the enzyme by mixed mode of inhibition. This in-

hibition strategy and encapsulated hydrophobic curcumin inside the cage were used to control the growth of methicillin-resistant *Staphylococcus aureus*.

A. Mondal, I. A. Bhat, S. Karunakaran, Dr. M. De\*

1 – 7

Supramolecular Interaction of Molecular Cage and  $\beta$ -Galactosidase: Application in Enzymatic Inhibition, Drug Delivery and Antimicrobial Activity

